Light Metals 2011 *Edited by: Stephen J. Lindsay*
TMS (The Minerals, Metals & Materials Society), 2011

Towards a design tool for self-heated cells producing liquid metal by electrolysis

Sophie Poizeau, Donald R. Sadoway

Department of Material Science and Engineering, Massachusetts Institute of Technology, Cambridge, Massachusetts 02139-4307, USA

Keywords: finite element modeling, Hall-Héroult cell, electrolysis, sideledge, turbulent flow, heat transfer coefficient

Abstract

As part of an effort to assess the technical feasibility of producing metals by molten salt electrolysis, a design tool is under development for the purposes of estimating the threshold cell size and current for self-heating operation. To make the model broadly applicable to the production of different metals, two major issues must be addressed. First, accurate values of the heat transfer coefficient are required in order to model the position of the ledge. In the Hall-Héroult cell, the heat transfer coefficient is determined experimentally from industrial operation, an approach that is not possible for a cell that has never been built. Second, thorough treatment of transport phenomena in the cell involves solving the equations for liquid and gas flows simultaneously; however, the methods used to model the turbulent flows in the Hall-Héroult cell are usually not well coupled.

Introduction

As seen on Figure 1, the Hall-Héroult cell is composed of three main parts: the carbon anode at the top, the electrolytic bath in the middle and the aluminium pool at the bottom. The electrolyte contains the alumina dissolved into enriched cryolite. Because of the difference in density between the liquid aluminium and molten electrolyte, the liquids are self-segregated: the aluminium produced goes to the bottom of the cell. Carbon dioxide bubbles are produced at the electrolyte/anode interface. Frozen electrolyte forms a sideledge against the walls.

There is an optimum thickness for the sideledge: too thin fails to protect the wall against chemical attack; too thick reduces useful electrolyte capacity. This equilibrium can be optimized through determination of the temperature profile. The electric current imposed across the cell has two main functions: producing aluminium but also keeping the liquids in the cell in the molten phase at 960°C. The temperature is not homogeneous throughout the cell: the temperature of the sidewalls varies from 100 to 300°C, the lowest temperatures being observed at the bottom and top of the cell, the highest temperature at the electrolyte level [1].

In the process of designing a new process for metal production by molten oxide electrolysis (MOE) [2], the well-studied Hall-Héroult process serves as an excellent starting point. MOE has become the focus of attention for its potential for carbon-free iron making as well as in situ generation of oxygen from lunar regolith [3]. To design a self-heating cell, a tool is needed to optimize parameters such as the size of the cell, the current density, the interelectrode gap and the composition of the electrolyte. The first interest would be to obtain a temperature profile that provides a similar crust to what is achieved in Hall-Héroult cells. To validate this design tool, we would compare its solution for the bath temperature of a known process, namely Hall-Héroult.

Existing models: operating tools adapted to the thermal management of the Hall-Héroult cell

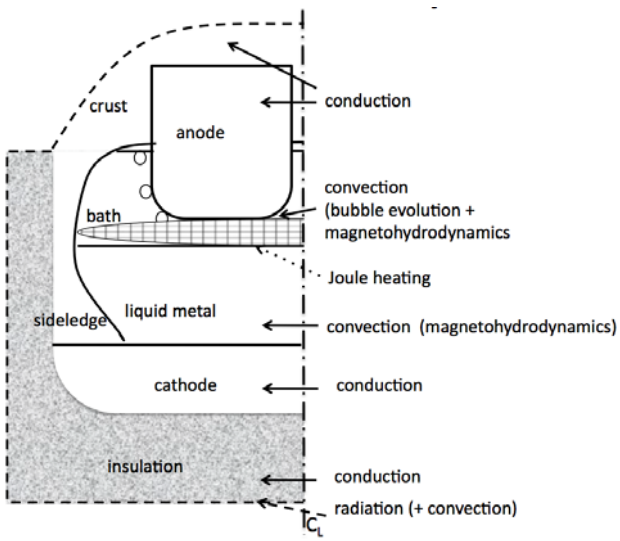

Figure 1: heat transfers at steady state

In this part, the authors will focus on the modeling work reported in the literature to evaluate to which extent it could be transposed to other chemistries. The heat generation (grid pattern on Figure 1), the heat flows inside the cell and finally the heat loss (dashed line) at the boundaries will be evaluated. The ledge position is closely

related to the consumption of additional heat to go from liquid to solid state (or vice versa), and will be treated with the heat generation.

1. Heat generation

Joule heating Heat is produced in the Hall-Héroult cell through Joule heating. The two parameters that determine the importance of heat creation are the electrical resistivity and the current density. The electrolyte is the poorest conductor compared to the other cell components where current flows (through the anodes and the cathode). Indeed, the conductivity of the electrolyte is about 200 S/m [4] in a pseudo steady state, while the conductivity of aluminium is 4 10^6S/m [5] and the conductivity of carbon in the anode and cathode is about $10^4 - 10^5$ S/m. Therefore, the interelectrode gap determines the amount of heat produced and must be kept constant during the operation of the cell to keep the temperature constant. The interelectrode gap is usually 4 to 5 cm large to ensure that the fluids are at 960℃.

Sideledge formation The sideledge formation is important to be taken into account to know its position and where the thermal properties of the bath are discontinuous. The sideledge present in the Hall-Héroult cell is crucial to the good functioning of the process for two main reasons: the sideledge (1) protects the sidewall from the combined action of high temperature, oxidizing cell gases, molten aluminium, and the fluoride-based bath and (2) limits heat losses. The composition of the sideledge is not uniform from the top of the electrolyte to the bottom of the aluminium pool. Indeed, at the bath level, the sideledge is due to the solidification of the bath, and the interface is defined by the melting point of the bath, while at the metal level a thin film of bath saturated with alumina of the order of millimeters covers the sideledge [6]. The mechanism of formation of the top and the bottom ledge is completely different, even though heat transfer coefficients are usually used in both cases.

The literature is prolific concerning heat transfer coefficients for the bath-ledge interface. Chen [7] listed twelve different papers, giving heat transfer coefficients in the range of 116 to 1820 W/m^{2}K. The main reason for this diversity is the dependence of the heat transfer coefficient on experimental conditions. For this reason, authors have developed experimental functions depending on those experimental conditions. Solheim [8] and Khoklov [9] recognized the impact of the gas flow rate, the immersion depth and the anode sideledge distance on the heat transfer coefficient. Nazeri [10] and Dupuis [11] used a function of the bulk fluid velocity in the immediate vicinity of the ledge, depending linearly [11; 12; 10] or on the square root of the velocity [11]. Even if the authors do not seem to agree on the value and the dependence of this coefficient, their results match very well to the reality. Indeed, the authors were able to tune their functions. However, because of this essential tuning, it makes those models non-transferable to other chemistries for which the cell does not exist. Severo [13] used the law of the wall determined experimentally by Kader [14] in the case of a temperature field developed in a turbulent boundary layer along a smooth wall. This complex law has the advantage of being transferable to other chemistries. However, it used the temperature of the wall and the temperature near the wall, whose determination was left unexplained.

The metal-ledge interface has not been studied as extensively as the bath-ledge interface and is usually treated similarly to the bath-ledge interface, with a heat transfer coefficient. However, as Solheim mentioned [6], the sideledge is separated from the metal pool by a thin bath film that does not have the same composition as the bulk of the bath. Its temperature is therefore not fixed at a melting point temperature. In all the simulations presented [11; 9; 13], the heat flux determined to get the position of the ledge is the product of the heat transfer coefficient and the superheat temperature, defined as the temperature difference between the temperature of the bath and the melting point of the bath. It is not clear how the superheat can be used to describe an interface that is not at a defined temperature.

2. Heat distribution inside the cell

Inside the cell, the heat is distributed everywhere by conductive heat transfer, as well as convective heat transfer in the molten aluminium and cryolite.

Convection This is the dominant heat transfer mode in the electrolyte and liquid aluminium. The heat motion in the case of the Hall-Héroult cell is due to:

- natural convection via buoyancy force.
- forced convection, via gas bubble flow in the cryolite, or magnetic forces in fluids that are electrically conductors (molten aluminium and cryolite). To calculate the velocity, the heat equation has therefore to be coupled with the Navier-Stokes equation. The forced convection contributions are developed below.

Gas bubbles

Anode gas evolution in aluminium reduction cells is an important driver of electrolyte flow and alumina mixing. In the cryolite, the values of the velocity due to gas bubbles and of the velocity due to the magnetic forces [15] are similar, while the orientation is different. Therefore it is also necessary to calculate the impact of the bubbles for the sideledge determination.

In the literature, several methods are used to determine the velocity of the fluid. Solheim [16] determines the mean velocity of the bubbles in a water-air full scale prototype, fitting a dimensionless equation with the data. The result outlines the role of all the physical parameters, such as the distance from the liquid metal, the dynamic viscosity and the slope of the anode. These data however do not indicate the direction of the flow and therefore could not be used as base flow in the solution of the global velocity in a full computational model.

The bubbles can be tracked individually. Johansen [17] undertook this first in the case of bubble stirred ladles. He treated the problem from a hydrodynamic view, considering two phases, the electrolyte as a primary phase, introducing the k-ϵ method for turbulent flow in Fluent, and the bubbles as a secondary dispersed phase with an approximate drag coefficient for spherical bubbles. In this method, turbulent viscosity is expressed as a function of kinetic energy and the dissipation rate of the turbulence energy, two dependent variables adding two additional transport equations. The bubble drag term is characterized by a relative Reynolds number and a drag coefficient. Fraser [18] reused this method in 2D, with a slightly different drag force coefficient in the case of the Hall-Héroult cell, as well as Purdie [19] in 3D, who did not specify the drag force coefficient he used in Fluent. In those two last cases, the maximal velocity calculated was 44 and 33 cm/s respectively. Solheim [15] also used a two-phase approach to model the fluid flow, using the k-ϵ turbulence model as well and a slightly different drag force term from Fraser and Johansen. For an inclination angle of 2° he calculated a maximum velocity of 5.8 cm/s away from the center of the anode, which is consistent with experimental data for Hall-Héroult cell, and a maximum velocity of 30 cm/s.

In all those methods, only two phases were considered: the gas and the electrolyte. The liquid metal is not considered. Indeed, this Lagrangian tracking method is only suitable to two phases in the way the equations are defined.

Magnetohydrodynamics

Magnetohydrodynamics constitute the major cause of fluid flow in the molten aluminium since no bubble flow is active there. They are also a major contribution of the fluid flow in the cryolite. Due to the fact that the anode area is smaller than the cathode area, the current diverges in the cell and creates a high magnetic field. It is usually on the order of 10^{-2} T. Because the molten aluminium and the cryolite are both conducting fluids, the combination of the current and the magnetic field causes electromagnetic forces, also called Lorentz forces. Those forces are responsible for the metal and bath flow, as well as for the metal-bath interface deformation. The typical flow velocity of the cell is 0.1 m/s while the interface is about 8 cm higher in the middle than on the sides of the cell [20].

Two main challenges need to be overcome to get a proper velocity profile inside the cell and be able to get a right convective heat flow in a finite element simulation. The first one is the determination of the moving interface between two fluids, while the second one is the treatment of turbulent flows.

Simulation of the moving interface

To model the moving interface, several methods are used as found in the literature.

If a fixed mesh is used, the interface is the line where the volume fractions of both fluids are equal. This line does not go through any particular nodes of the mesh. It has a finite width, along which the properties change continuously from the cryolite to the aluminium phase. For instance, most software has the ability to use the so-called method of phase field. This method solves the Cahn-Hilliard equation and is usually used to model phase separation. Severo [20] used a similar method provided in Ansys CFX. Not only such methods are computationally expensive, since the mesh at the interface has to be very small, but Severo noticed that his results were not good compared to other methods if the air gap on the top on the cryolite is not included. But this increases of course the complexity of the problem, since two interfaces and three fluids have to be taken into account at the same time.

If a moving mesh is used, the interface is located at the common boundary of two finite elements/volumes, one having the properties of cryolite, the other having the properties of aluminium. This method is usually used in combination with the shallow layer approximation, also called St Venant approach [21; 22; 20], which is justified in the case of the Hall-Héroult cell. Indeed, the vertical dimensions of the fluids are considered small compared to the horizontal dimensions of the cell and the interface wave amplitude is small compared to the depth. The St Venant approach neglects the vertical dependency for the velocity while approximating the pressure by the hydrostatic pressure [22]. It gives fast results consistent with experimental ones[20].

Treatment of the turbulence in aluminium and cryolite flows

As seen above, some artifacts are usually necessary to be able to get a solution in modeling when turbulent flows are present, increasing the viscosity of the fluid to take

into account the effects of the turbulence. We saw in the case of gas bubble flow that the cryolite flow could be solved using k-ϵ method. Severo tried to use this in the case of a three-phase (aluminium, cryolite, air on the top) model and it led to an underestimation of the displacement of the interface by 4 cm (50%). Indeed, the k-ϵ method often shows poor agreement in the description of rotating flows dominated by body forces, which is the case here. Therefore, other methods are used to treat the turbulence of the flows in the case of the Hall-Héroult cell.

The most common way to model turbulence is by assuming that it is purely diffusive. The turbulent viscosity is considered to be a constant and called the eddy viscosity. This viscosity is usually around 0.5-1 Pa.s in the case of the Hall-Héroult cell in both fluids [20]. This represents 1000 times more than their real viscosity (about 0.8 mPa.s for aluminium and 3 mPa.s for the bath). Severo [20] and Wahnsiedler [23] used this method. The turbulent viscosity is determined by tuning the model.

The last method used is the k-ω turbulence method [24], in which the transport of the dissipation per unit turbulent energy is modeled instead of the dissipation itself, as it is the case in the k-ϵ method. The results [21] are consistent with those from Severo [20] for the interface shape. The velocity profile is similar to those from other simulations [25; 23] with values around 10 cm/s.

To conclude this part on magnetohydrodynamics, the floating grid seems to be preferable for models already complex enough, and the k-ω method to treat the turbulence would allow the user not to depend on measured quantities. However, the combination of magnetohydrodynamics with bubble flow is challenging, since the models for bubble flow are using Lagrangian tracking of bubbles, a gas-liquid phase model and the method to deal with the turbulence is k-ϵ, that does not work well for magnetohydrodynamics [20].

3. Heat losses

The heat losses in the Hall-Héroult cell are typically distributed equally through the top and sides of the cell, and a small amount through the bottom (less than 10%). The heat can be lost at the boundaries through convective or radiative heat transfer. Radiative heat transfer is the main factor of dissipation of energy, since the emissivity of the sideblocks is about 0.8 and the temperature gradient is large. Haugland [1] calculated that, for a wall temperature of 350°C and an ambient temperature of 30°C, radiative heat is equivalent to convective heat with a transfer coefficient of 23 W/m^2K , while the heat transfer coefficient due to pure convection is 5 W/m^2K.

Other needs for other problem: design tool

Experimental tuning

In this article, the authors have pointed out several coefficients that are determined experimentally: the heat transfer coefficient for the ledge, the superheat (difference of temperature between the bath temperature and the melting point of cryolite), the drag coefficient due to bubble flow, increased viscosity of the fluids to model the turbulence of the flows. Those parameters, such as the heat transfer coefficients and the superheat necessary for the sideledge determination, depend on the configuration of the cell [26], and are therefore unknown for unbuilt cells with different chemistries. This shows the difference in the requirements to get a good design tool versus operating tool.

Fully coupled model to get a temperature profile

The authors have shown that to evaluate the convective heat transfers correctly, the most problematic features are the velocity (involving bubble and magnetohydrodynamic flow) and the determination of the ledge.

Even if each part can be solved separately, the combination of those solutions may not give a reasonable answer. Indeed, the experimental constants used to solve those problems are usually experimentally determined while other phenomena are active, even if those phenomena are not modeled simultaneously. For instance, for most models of the ledge, no bubble flow is involved in the simulation [9], while the bubble flow (rate but also direction) has a large impact on the shape of the ledge [8]. This means that the bubble flow contribution is included in the heat transfer coefficient to get results consistent with experimental data [9]. Therefore, if the bubble flow would be added on top of this heat transfer coefficient, the contribution of the bubbles would be overestimated.

Moreover, the methods used to model one feature are not easily compatible with other methods. For instance, the determination of the velocity of the bath flow would need at least the treatment of four phases at the same time: the carbon dioxide bubbles, the cryolite, the aluminum, the sideledge (which could be divided in two), and eventually the gas on top of the channels. This is a huge challenge for the existing software. Another example is the treatment of the turbulence of those flows. The bubble flow is usually solved using the k-ϵ method, while this does not work for the magnetohydrodynamics [20]. A common way to solve turbulence in molten cryolite due to both bubble flow and magnetohydrodynamics needs to be found.

Other approach for the sideledge determination

The sideledge at the level of the electrolyte is due to the solidification of the bath, and the interface is defined by the melting point of the bath. In the approach used in the literature reviewed, a heat transfer coefficient and/or the superheat are used as parameters to evaluate the heat needed by the ledge to melt and the position of the ledge. Also, two phenomena happen at the liquid-solid interface: dissipation of energy and zero velocity in the solid phase. While the dissipation of energy can be modeled in the current literature of the Hall-Héroult cell models by those heat transfer coefficients, this method alone does not treat the zero velocity in the ledge.

Another approach that could allow the model to depend less on measured coefficients in the context of generalization to other chemistries would be to treat this problem as a phase transition from solid to liquid. Several methods are used to model phase transition, treating the two phenomena (latent heat effects and zero velocity) at the same time. To treat the energy dissipation/production at the interface, authors specialized in phase transition use mostly the enthalpy source method [27; 28], where the latent heat is incorporated in the heat equation as a source term, or the heat capacity method, where the latent heat is incorporated into the heat capacity [29]. To treat the zero velocity inside the solid phase, most authors assume a very large viscosity inside the solid phase [30; 29], or an artificial force that opposes the force applied to the fluid that provokes its movement [27; 28]. The usual drawback to those methods is that they require a really fine mesh at the interface, but they could be an interesting alternative to the empirical methods used in most articles reviewed.

Preliminary results

A first model of the Hall-Héroult cell was built following the recommendations of the first parts of the article, using Comsol Multiphysics v3.5a. The goal of this preliminary model was to determine the limits of simple modeling to determine the temperature inside the electrolyte in pseudo-steady state using only measured properties of the separate components used to built a cell in the industry. A 2D model was built to simplify the situation.

Internal heat transfers limited to conduction

In this first model, emphasis was placed on the impact of the boundary conditions. The heat source was determined by Joule heating, while the sinks were determined taking into account radiative and convective heat transfers. The outside temperatures to solve the boundary conditions were 160°C for the top of the cell, 60°C on the sides and 30°C at the bottom. The convective heat transfers were varied but without much impact on the solution since the radiative heat transfers were dominant, which was consistent with Haugland [1]. In this model, the variation of the properties of the bath with temperature (to model the ledge vs. liquid electrolyte) was taken into account using a step function.

The temperature of the liquid phases is obviously not correct, but the temperature of the solid phases is not too far from realistic temperatures. In particular, the outside temperatures are about 75-100°C as can be seen in Figure 2.

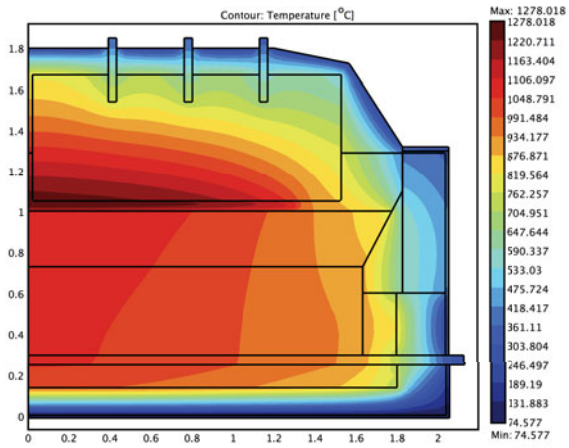

Figure 2: Steady state temperature with internal conductive heat transfers only

Natural convection in liquid aluminium

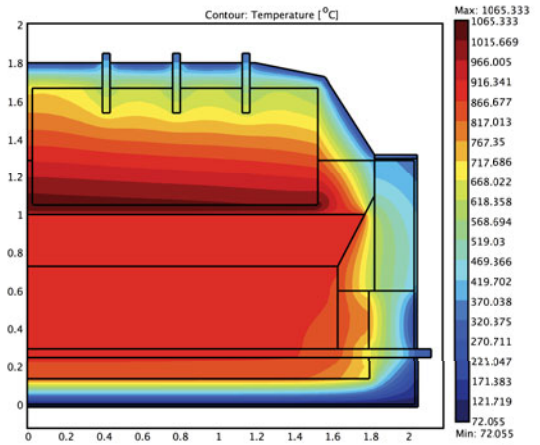

Figure 3: Steady state temperature with convection in aluminium

As a next step, the natural convection in the liquid alu-

minium was added. It is interesting to notice that even if the dominant convective flows due to forced convection were not present, the temperature of the aluminium phase homogenizes quickly (about 100 s), reaching a steady state after 500,000 s. The temperature in the aluminium is about 880℃. There are too many missing contributions (particularly the convection in the electrolyte) to draw conclusions about temperature discrepancies.

Limitations of this preliminary model

The limitations of the preliminary model were recognized when couplings of fluid flows or of phase transition with convection were tried using Comsol. When a phase field method was used to model the liquid-liquid interface, the number of elements was too large to get a solution on a large scale while on a smaller scale the proportion of the volumes were not conserved. When the liquid-solid phase transition was coupled with convection, it was not possible to reproduce the simulation of the melting of n-octadecane as published successfully in the literature [31] and known to be consistent with experiment [32].

Acknowledgements

The authors thank Dr. Alton Tabereaux and Dr. Adam Powell for their advice in this work, supported by the American Iron and Steel Institute and NASA.

References

[1] Haugland, E., Borset, H., Gikling, H., and Hoie, H. (2003) In Light Metals : pp. 269 – 76.

[2] Sadoway, D. R. (1995) *Journal of Materials Research* **10(3)**, 487 – 492.

[3] Sibille, L. (2009) In 47 th AIAA Aerospace Sciences Meeting : pp. Paper AIAA 2009–659.

[4] Hives, J., Thonstad, J., Sterten, A., and Fellner, P. (1994) In Light Metals : pp. 187 – 194.

[5] Brandt, R. and Neuer, G. (2007) *International Journal of Thermophysics* **28(5)**, 1429 – 1446.

[6] Solheim, A. (2006) In Light Metals : pp. 439 – 43.

[7] Chen, J. J. (1994) *JOM* **46(11)**, 15 – 19.

[8] Solheim, A. and Thonstad, J. (1984) *Journal of Metals* **36(3)**, 51 – 55.

[9] Khokhlov, V. A., Filatov, E. S., Solheim, A., and Thonstad, J. (1998) In Light Metals : pp. 501 – 506.

[10] Nazeri, H., Utigard, T., and Desclaux, P. (1994) *Light Metals* pp. 543–559.

[11] Dupuis, M. and Bojarevics, V. (2005) In Light Metals : pp. 449 – 54.

[12] Dupuis, M. (2002) In CIM : Canadian Institute of Mining, Metallurgy and Petroleum.

[13] Severo, D. S. and Gusberti, V. (2009) In Light Metals : pp. 557 – 562.

[14] Kader, B. (1981) *Int. J. Heat Mass Transf. (UK)* **24(9)**, 1541 – 4.

[15] Solheim, A., Johansen, S., Rolseth, S., and Thonstad, J. (1989) *J Appl Chem* **19(5)**, 703 – 712.

[16] Solheim, A., Johansen, S., Rolseth, S., and Thonstad, J. (1989) In Light Metals : pp. 245 – 252.

[17] Johansen, S. and Boysan, F. (1988) *Metallurgical transactions. B, Process metallurgy* **19(5)**, 755 – 764.

[18] Fraser, K., Taylor, M., and Jenkin, A. (1990) In Light Metals : pp. 221 – 226.

[19] Purdie, J. (1993) In Light Metals : pp. 355 – 360.

[20] Severo, D. S. (2008) In Light Metals : pp. 413 – 418.

[21] Bojarevics, V. and Pericleous, K. (2009) In Light Metals : pp. 569 – 574.

[22] Gerbeau, J.-F. (2006) Mathematical methods for the magnetohydrodynamics of liquid metals, Oxford University Press, .

[23] Wahnsiedler, W. (1987) In Light Metals : pp. 26 – 287.

[24] Bojarevics, V. (2004) *Metallurgical transactions. B, Process metallurgy* **35(4)**, 785 – 803.

[25] Evans, J. (1981) *Metall. Trans. B, Process Metall. (USA)* **12B(2)**, 353 – 60.

[26] Dupuis, M. and Haupin, W. (2003) In Light Metals : pp. 255 – 62.

[27] Brent, A., Voller, V., and Reid, K. (1988) *Numer. Heat Transf. (USA)* **13(3)**, 297 – 318.

[28] Voller, V. and Prakash, C. (1987) *Int. J. Heat Mass Transf. (UK)* **30(8)**, 1709 – 19.

[29] Morgan, K. (1981) *Comput. Methods Appl. Mech. Eng. (Netherlands)* **28(3)**, 275 – 84.

[30] Ma, Z. and Zhang, Y. (2006) *International Journal of Numerical Methods for Heat and Fluid Flow* **16(2)**, 204 – 225.

[31] Cao, Y. and Faghri, A. (1990/08/) *Trans. ASME, J. Heat Transf. (USA)* **112(3)**, 812 – 16.

[32] Okada, M. (1983) In ASME-JSME Thermal Engineering Joint Conference Proceedings. volume **1**, : pp. 281 – 288.